Dyes and Pigments 95 (2012) 392–399

Contents lists available at SciVerse ScienceDirect

Dyes and Pigments

journal homepage: www.elsevier.com/locate/dyepig

Design, synthesis and evaluation of redox, second order nonlinear optical properties and theoretical DFT studies of novel bithiophene azo dyes functionalized with thiadiazole acceptor groups

M.Cidália R. Castro [a], Peter Schellenberg [b], M. Belsley [b], A.Maurício C. Fonseca [a], Sara S.M. Fernandes [a], M.Manuela M. Raposo [a,*]

[a] Center of Chemistry, University of Minho, Campus de Gualtar, 4710-057 Braga, Portugal
[b] Center of Physics, University of Minho, Campus de Gualtar, 4710-057 Braga, Portugal

ARTICLE INFO

Article history:
Received 10 April 2012
Received in revised form
10 May 2012
Accepted 15 May 2012
Available online 23 May 2012

Keywords:
Heterocyclic azo dyes
Thiadiazole
Auxiliary donor/acceptor heterocycles
Hyper-Rayleigh scattering (HRS)
Density functional theory (DFT)
Nonlinear optical (NLO) materials

ABSTRACT

Two series of novel thermally stable second-order nonlinear optical (NLO) heterocyclic azo dyes **4**–**5** have been designed and synthesized. The two series of compounds were based on different combinations of acceptor groups (thiadiazole or arylthiadiazole electron-deficient heterocycles) linked to bithiophene which acts at the same time as a donor group and as a π-conjugated bridge. The solvatochromic behavior of azo dyes **4**–**5** was investigated in several solvents of different polarity, while their thermal stability was evaluated using thermogravimetric analysis. Optimized ground-state molecular geometries and an estimation of the lowest energy single electron vertical excitation energies in DMF solutions were obtained using density functional theory (DFT). Their redox properties were studied by cyclic voltammetry, while hyper-Rayleigh scattering (HRS) was employed to evaluate their second-order nonlinear optical properties. The measured molecular first hyperpolarizabilities and the observed electrochemical behavior showed variations for the different acceptor systems used (thiadiazole or arylthiadiazole) and were also sensitive to the electronic acceptor strength of the substituents (*R*) linked to thiadiazole or arylthiadiazole heterocycles. Donor–acceptor arylthiadiazole-bithienyl diazenes exhibit the most promising thermal (T_d = 237–305 °C) and solvatochromic ($\Delta\nu$ = 1117–2503 cm^{-1}) properties and second order nonlinear optical response (136–226 × 10^{-30} esu).

© 2012 Elsevier Ltd. All rights reserved.

1. Introduction

Heterocyclic azo dyes are versatile chromophores that can provide bright strong shades tunable for absorption over all of the visible spectrum [1]. For decades, they have been widely investigated mostly due to their application for coloring textiles and plastics or in general as dispersed dyes. More recently azo dyes bearing heterocyclic moieties such as thiophene, pyrrole and azoles have been used for multiple optical and electronic applications such as second harmonic generation, optical switching, chemosensing, and organic sensitized solar cells [2].

Due to their well established synthetic routes, they are well suited candidates for a systematic investigation of how NLO properties are affected by variations within their π-conjugated system. In the past years we have been exploring the ways in which the second order nonlinear response of these push–pull organic molecules can be improved by inclusion of different heterocycles within the π-electron bridge, using them both as a means of modulating the conjugation in the π-electron network and to change the electronic character of the charge transfer by acting as auxiliary donors or acceptors [3,4]. Previously we reported also other NLO-active heterocyclic chromophores bearing electron rich groups (thiophene, pyrole) linked to electron deficient heterocycles (benzothiazole, benzimidazole and phenanthroline) [5]. However, despite intensive theoretical and experimental activity it remains at present unclear what the right strategy will be to optimize NLO properties.

On the other hand, it is well known that push–pull systems bearing azole electron-deficient heterocycles can increase the quadratic molecular nonlinear optical response due to the electronegative nitrogen and sulfur atoms [6]. In this respect, five-membered diazoles, in particular thiadiazole, seems to be an appropriate acceptor moiety. It possesses two nitrogen atoms and

* Corresponding author. Tel.: +351 253 604381; fax: +351 253 604382.
E-mail address: mfox@quimica.uminho.pt (M.M.M. Raposo).

0143-7208/$ – see front matter © 2012 Elsevier Ltd. All rights reserved.
doi:10.1016/j.dyepig.2012.05.014

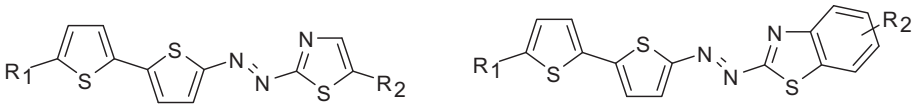

6 R_1 = H, MeO, EtO; R_2 = H, CH_3, CHO

7 R_1 = H; R_2 = H, CH_3

Fig. 1. Structure of bithienyl-thiazolyl **6** and benzothiazolyl diazenes **7** [3f,4d].

a sulfur atom with different electronic nature and represents a robust and stable heterocycle. Earlier studies on NLO-chromophores bearing thiadiazole heterocycle showed its potential application as second order nonlinear optical chromophores [7].

Our earlier studies concerning the evaluation of electronic and optical properties of heterocyclic azo dyes bearing thienylpyrrole [3] or bithiophene [4] π-conjugated bridges and simultaneously donor groups linked to thiazolyl- (**6**) or benzothiazolyl- (**7**) diazene acceptor moieties, (Fig. 1) reveal that their optical and redox properties can be modulated by varying the position of the heterocycle attachment to the diazene group, by altering the electronic nature of the groups substituted on the heterocyclic diazene system as well as by tuning the electronic acceptor strength of the heterocycle on the same diazene moiety.

In view of these findings and in continuation of our recent work concerning the synthesis and characterization of heterocyclic azo dyes as solvatochromic probes, second harmonic generators and photochromic systems [3,4] we report here on the synthesis and evaluation of optical (linear and nonlinear), redox and thermal properties of two series of heterocyclic chromophores consisting of newly synthesized (aryl)thiadiazolyldiazenes **4**–**5** bearing bithiophene spacers. Additionally, optimized ground-state molecular geometries and estimation of the lowest energy single electron vertical excitation energies in DMF solutions for the novel chromophores were obtained using density functional theory (DFT).

2. Results and discussion

2.1. Synthesis

Generally thiophene azo dyes are synthesized through azo coupling reaction of 2-aminothiophenes with arylamines [1a,8], however the difficulties of synthesizing 2-aminothiophenes are well known. In order to overcome these problems, we have recently developed a novel synthesis methodology for bithienyl diazenes using as coupling components 2,2′-bithiophene, 5-alkoxy- or 5-*N*,*N*-dialkylamino-2,2′-bithiophenes and (hetero)aryldiazonium salts [4a,b,d],

Consequently, 2,2′-bithiophene **1** has been used as coupling component together with thiadiazolyl **2a**–**c** and arylthiadiazolyl **3a**–**c** diazonium salts in order to prepare heterocyclic azo dyes **4**–**5** (Scheme 1). Diazotation of 2-amino-thiadiazole and 2-amino-arylthiadiazole derivatives with $NaNO_2$ in HCl (6 N) at 0–5 °C in water gave rise to the corresponding diazonium salts **2**–**3**, which reacted with bithiophene **1** in acetonitrile at 0 °C given thiadiazolyl diazenes **4**–**5** in fair to moderate yields (15–58%).

All the compounds were completely characterized by ^1H and ^{13}C NMR, IR, MS, EA or HRMS and the data obtained were in full agreement with the proposed formulation.

2.2. Redox properties

The redox properties of bithiophene azo dyes **4**–**5** were studied by cyclic voltammetry in DMF containing tetrabutylammonium tetrafluoroborate (1 mmol dm^{-3}) as the supporting electrolyte. Table 1 lists the reduction and oxidation onsets and the electrochemical band gap values, using ferrocene as reference.

All molecules showed a donor–acceptor character with reversible reductions and irreversible oxidation processes. The irreversible oxidation process is associated with the oxidation of the thiophene moiety. These results are consistent with previous electrochemical studies of other thiophenes derivatives [3a,c,d,9]. The values for the oxidation process are shifted to more anodic potentials when stronger acceptor substituent groups are introduced in thiadiazole and arylthiadiazole moieties. All bithiophene azo dyes **4**–**5** bearing a thiadiazole and arylthiadiazole acceptor group linked to the diazene group through position 2 exhibited two one-electron reversible reductions indicating a high electron affinity of the chromophores (Fig. 2).

The one-electron stoichiometry for these reduction processes is ascertained by comparing the current heights with known one-electron redox processes under identical conditions [3a]. For all compounds, the two reduction processes are associated with the reduction of the (hetero)aromatic azo moiety. The introduction of an arylthiadiazole acceptor group linked to the azo bridge through position 2 (compound **5a**) could slightly decrease the reduction potentials (compared to the corresponding thiadiazole derivative **4a**) while increasing the oxidation potentials, suggesting a higher electron-accepting ability of compound **5a**. It was also observed for all compounds, that the reduction potential values of the first and second processes are influenced by the acceptor electronic strength of the substituent on the thiadiazole ($^1E_{pc}$ for **4a** < $^1E_{pc}$ for **4b** < $^1E_{pc}$ for **4c**) and arylthiadiazole rings ($^1E_{pc}$ for **5a** < $^1E_{pc}$ for **5b** < $^1E_{pc}$ for **5c**). Therefore, the substitution on the aryl ring of the arylthiadiazole system by fluoro (**5b**) or nitro (**5c**) groups results in a moderate decrease of the reduction potentials ($^1E_{pc} = -1.04$ V for **5b** and $^1E_{pc} = -0.95$ V for **5c**) when compared to the reduction potential obtained for the unsubstituted derivative (**5a**,

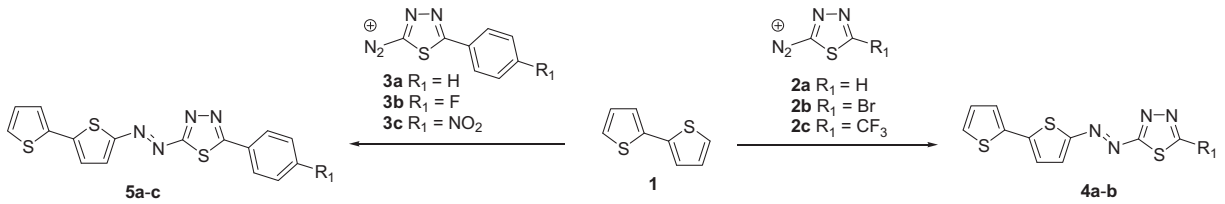

Scheme 1. Synthesis of bithienyl diazenes **4**–**5** trough azo coupling reaction of 2,2′-bithiophene **1** with thiadiazolyl diazonium salts **2**–**3**.

Table 1
Electrochemical data for compounds **4**–**5**.

Compound	Reduction[a]				Oxidation[a]	Band gap[c] (eV)
	$-^{1}E_{pc}$ (V)	ΔE^{b} (mV)	$-^{2}E_{pc}$ (V)	ΔE^{b} (mV)	E_{pa} (V)	
4a	1.09	63	1.96	64	0.95	2.04
4b[d]	0.96	63	1.97	63	0.97	1.93
4c	0.84	61	1.67	70	0.99	1.83
5a	1.05	63	1.89	63	0.98	2.03
5b	1.04	62	1.87	61	1.01	2.04
5c	0.95	61	1.46	63	1.04	1.99

[a] Measurements made in dry DMF containing 1.0 mM in each compounds and 0.10 M $[NBu_4][BF_4]$ as base electrolyte at a carbon working electrode with a scan rate of 0.1 V s^{-1}. All *E* values are quoted in volts *vs.* the ferrocenium/ferrocene -couple. E_{pc} and E_{pa} correspond to the cathodic and anodic peak potentials, respectively.
[b] $\Delta E = |E_{red} - E_{ox}|$.
[c] $E_{HOMO} = -(4.39 + E_{ox})$ (eV) and $E_{LUMO} = -(E_{red} + 4.39)$ (eV).
[d] Additional cathodic irreversible process was observed at −1.77 V *vs.* fc^{+}/fc, attributed to the loss of bromide [11].

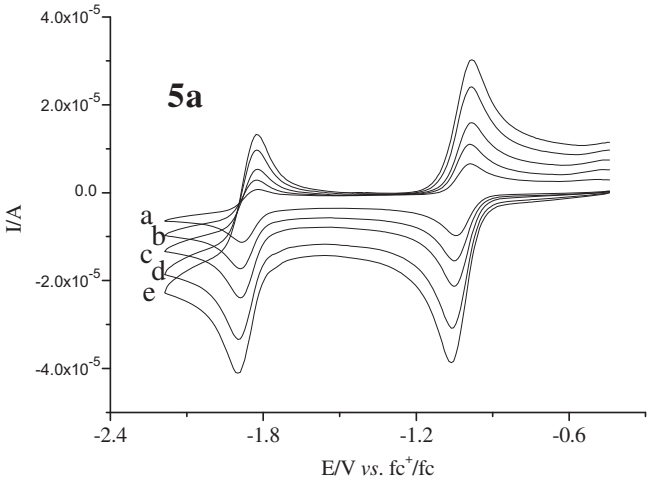

Fig. 2. Cyclic voltammograms for the reduction steps of compound **5a** (1.0×10^{-3} mol dm^{-3}) in DMF, 0.1 mol dm^{-3} $[NBu_4][BF_4]$ at a vitreous carbon electrode, between −0.5 V and −2.20 V *vs.* fc^{+}/fc, scan rate at 0.02 (a), 0.05 (b), 0.10 (c), 0.20 (d) and 0.30 (e) V s^{-1}.

$^{1}E_{pc} = -1.05$ V). On the other hand a higher decrease on the reduction potential were observed in the case of thiadiazole azo dyes (e.g. **4c**, $^{1}E_{pc} = -0.84$ V and **4a** $^{1}E_{pc} = -1.09$ V). The electrochemical band gaps were calculated as described previously [10] from the potentials of the anodic and cathodic processes (Table 1). The efficient donor–acceptor conjugation leads to a lowering of the HOMO and the LUMO levels in compounds **4** and **5**, revealing efficient coupling between the bithiophene spacer and thiadiazolyl or arythiadiazolyl-diazene acceptor groups.

2.3. Optical properties

(Aryl)thiadiazole azo dyes **4**–**5** showed good solubility in common polar and non-polar organic solvents such as diethyl ether, dioxane, ethanol and DMSO.

All chromophores exhibit broad and intense CT absorptions in the region of 475–508 nm in dioxane. Thiadiazole being an electron-deficient five-membered heteroaromatic ring, will act as acceptor group and will exhibit also an auxiliary acceptor effect when linked to withdrawing groups [6a–c]. Moreover, due to a larger electronic delocalization, (aryl)thiadiazole azo dyes **5** exhibit bathochromic shifts when compared to the corresponding thiadiazole derivatives **4** (Fig. 3). The acceptor electronic strength of

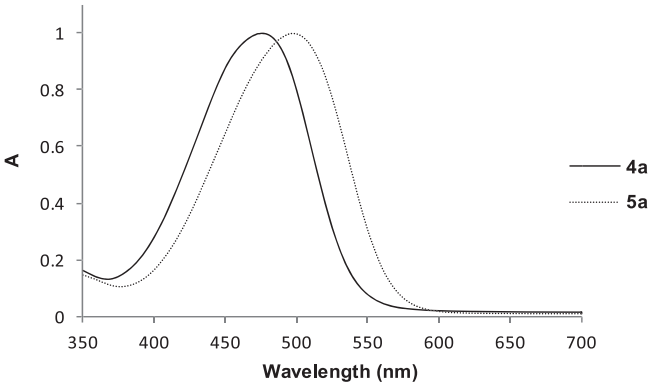

Fig. 3. UV–visible absorption normalized spectra of compounds **4a** and **5a** in dioxane at room temperature.

the groups substituted on thiadiazole or on the arylthiadiazole heterocycles have a significant effect on the electronic absorption property of compounds **4** and **5**. Therefore, azo dyes **4c** and **5c** exhibited a red-shifted λ_{max} (21 and 12 nm, respectively) with respect to the unsubstituted derivatives **4a** and **5a**.

The wavelength maxima λ_{max} of compounds **4**–**5** in four solvents, are summarized in Table 2 and were compared with the π^{*} values for each solvent, as determined by Kamlet and Taft [12]. Thiadiazole azo dyes **4** ($\Delta\upsilon_{max} = 926$–$1216$ cm^{-1}) and **5** ($\Delta\upsilon_{max} = 950$–$2503$ cm^{-1}) exhibited positive solvatochromism from diethyl ether to DMSO, suggesting the good optical nonlinearities of these chromophores (Fig. 4).

The molecular first hyperpolarizabilities β of heterocyclic diazenes **4**–**5** were measured by hyper-Rayleigh scattering (HRS) method [13] at a fundamental wavelength of 1064 nm of a laser beam. Dioxane was used as the solvent, and the β values were measured against a reference solution of *p*-nitroaniline (*p*NA) [14] in order to obtain quantitative values, while care was taken to properly account for possible fluorescence of the dyes (see experimental section for more details). The static hyperpolarisability β_0 values [15] were calculated using a very simple two-level model neglecting damping. They are therefore only indicative and should be treated with caution (Table 3).

From Table 3 it is apparent that the increase of the acceptor strength of the substituent on 5-position of the thiadiazole ring (dyes **4a**–**c**) resulted in a significant resonant enhancement, with enhanced β values accompanied by a red-shifted absorption maxima (e.g. **4a**, R = H, λ_{max} 475 nm, $\beta = 153 \times 10^{-30}$ esu; **4c**, $R = CF_3$, λ_{max} 496 nm, $\beta = 221 \times 10^{-30}$ esu). Also noteworthy is the effect of the electronic nature of the group that substitutes the aryl ring at 4-position for compounds **5a**–**c**. As expected the increase of the acceptor strength of the NO_2 group (**5c**) compared to H (**5a**)

Table 2
Solvatochromic data [λ_{max} (nm) and $\Delta\upsilon_{max}$ (cm^{-1}) of the charge-transfer band] for bithiophene azo dyes **4**–**5** in 4 solvents with π^{*} values by Kamlet and Taft [12].

Compound	Solvent (π^{*})							
	Diethyl ether (0.54)		Ethanol (0.54)		1,4-Dioxane (0.55)		DMSO (1.00)	
	λ_{max} (nm)	ν_{max} (cm^{-1})	λ_{max} (nm)	ν_{max} (cm^{-1})	λ_{max} (nm)	ν_{max} (cm^{-1})	λ_{max} (nm)	ν_{max} (cm^{-1})
4a	466	21,459	483	20,704	475	21,053	494	20,243
4b	487	20,534	498	20,080	490	20,408	510	19,608
5a	487	20,534	504	19,841	496	20,161	515	19,417
5b	491	20,367	502	19,920	498	20,080	515	19,417
5c	495	20,202	518	19,305	508	19,685	565	17,699

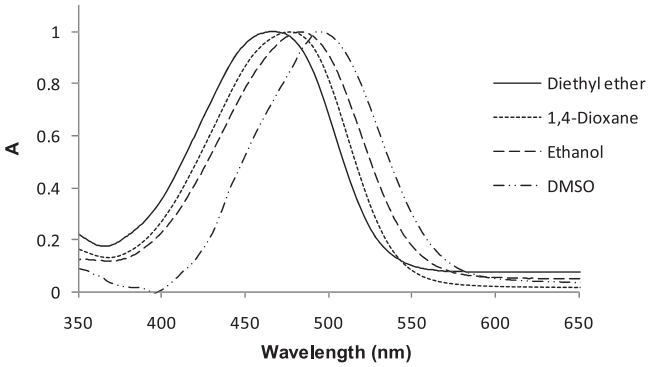

Fig. 4. UV–visible absorption normalized spectra of compound **4a** in four solvents of different polarity (diethylether, dioxane, ethanol and DMSO) at room temperature.

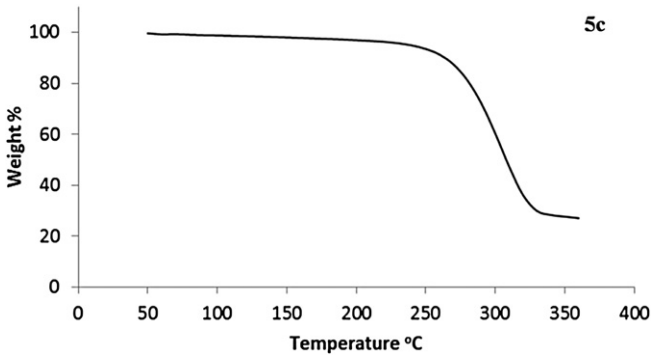

Fig. 5. Thermal analysis data for compound **5c** through TGA recorded under a nitrogen atmosphere, measured at a heating rate of 20 °C min^{-1}.

results both in red-shifted absorption maxima (12 nm) and a resonance enhanced β value for arylthiadiazole azo dye **5c** ($\beta = 226 \times 10^{-30}$ esu).

Comparison of the β values for arylthiadiazole azo dye **5a** with thiadiazole azo dye **4a** also showed that the substitution of a thiadiazolyl-diazene for a arylthiadiazolyl-diazene acceptor moiety enhances the first order hyperpolarizability from 153×10^{-30} to 170×10^{-30} esu at 1064 nm, probably due a greater electronic delocalization. In the probable resonance structures, the distance between the charges in **5a** is longer compared to **4a**, which results in a greater electric moment of the first diazene, increasing the value of the molecular hyperpolarizability.

A comparison could also be made between dyes **4a** and **5a** and bithiophene thiazolyl azo dye (**6**, $R_1 = R_2 =$ H, $\lambda_{max} = 477$ nm in dioxane) and benzothiazolyl-diazene (**7**, $R_1 = R_2 =$ H, $\lambda_{max} = 493$ nm in dioxane) reported by us recently (Fig. 1) [4d]. The results obtained previously suggest that the electron-deficient thiazole and benzothiazole heterocycles have a larger acceptor strength than thiadiazole and arylthiadiazole systems. As a result β values of the thiazolyl- **6a** ($\beta = 172 \times 10^{-30}$ esu) and benzothiazolyl- **7a** ($\beta = 207 \times 10^{-30}$ esu) diazenes are larger than the corresponding values for thiadiazole (**4a**, $\beta = 153 \times 10^{-30}$ esu) and arylthiadiazole **5a** ($\beta = 170 \times 10^{-30}$ esu) dyes.

For optoelectronic applications, the thermal stability of organic materials is critical for device stability. For that reason the thermal properties of the chromophores **4**–**5** were investigated by thermogravimetric analysis under a nitrogen atmosphere, measured at a heating rate of 20 °C min^{-1} (Table 3). All chromophores are thermally stable with decomposition temperatures varying from 221 to 305 °C. In both series of derivatives the electronic nature of the group substituted on the 5-position of the thiadiazole ring (**4a**–**c**) or in 4-position of the aryl ring (**5a**–**c**) does seem to have some impact on the thermal stability of the compounds. Therefore, the nitro arylthiadiazolyl azo dye **5c** (Fig. 5) and the bromo substituted thiadiazolyl derivative **4b** are the most stable showing higher decomposition temperatures.

Arylthiadiazole azo dye **5a** exhibit also an improved stability by *ca* 26 °C compared to the corresponding thiadiazole derivative **4a**.

2.4. Theoretical calculations

Theoretical calculations were carried out using density functional theory to model the ground state molecular geometries and energies, the HOMO–LUMO energy gaps as well as the optical absorption spectra. The class of bithienyl-(aryl)thiadiazole azo dyes investigated here possess three rotatable single bonds present throughout the conjugated system indicated as A, B and C in (Fig. 6). However, these bonds may have a higher isomerization energy compared to isolated single bonds as they are part of the conjugated electronic system.

Therefore eight structurally distinct isomeric configurations are possible in thermal equilibrium [16,17]. Here, we use the nomenclature from [16] according to which *c* and *t* stands for *cisoid* and *transoid*, respectively. All calculations were performed using the

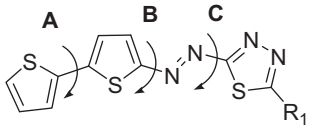

Fig. 6. Rotatable bonds within the conjugated system responsible for the different isomers.

Table 3
Experimental data for bithiophene azo dyes **4**–**5**.[a]

Heterocyclic azo dye	R_1	Yield (%)	λ_{max} (nm) (ε)	β^b (10^{-30} esu)	$\beta_0{}^c$ (10^{-30} esu)	$T_d{}^d$ (°C)
4a	H	19	475 (19,980)	153	25 ± 2.3	221
4b	Br	21	490 (36,410)	193	23 ± 1.8	244
4c	CF_3	15	496 (28,440)	221	23 ± 1	–
5a	C_6H_4	58	496 (23,400)	170	19 ± 1	237
5b	4-FC_6H_4	34	498 (36,140)	136	21 ± 1	248
5c	4-$NO_2C_6H_4$	16	508 (12,590)	226	15.4 ± 0.5	305
*p*NA	–	–	352	16.9 [14]	8.5	–

[a] Experimental hyperpolarizabilities and spectroscopic data measured in dioxane solutions.
[b] All the compounds are transparent at the 1064 nm fundamental wavelength.
[c] Data corrected for resonance enhancement at 532 nm using the two-level model with $\beta_0 = \beta\,[1 - (\lambda_{max}/1064)2][1 - (\lambda_{max}/532)2]$; damping factors not included 1064 nm [15].
[d] Decomposition temperature (T_d) measured at a heating rate of 20 °C min^{-1} under a nitrogen atmosphere, obtained by TGA.

Table 4
The energy values for the HOMO and LUMO and the HOMO–LUMO energy gap for each compound averaged over the results for the eight possible isomers as shown in Supplementary Table S1 for compound **4a**. The values given for $\Delta E_{max/min}$ refer to the spread between the largest and smallest values of energy obtained amongst the eight isomers of each compound.

	$E_{(HOMO)}$[a] DMF/eV	$E_{(LUMO)}$[a] DMF/eV	$\Delta E_{(HO-LU)}$[b] DMF/eV	$\Delta E_{max/min}$ DMF/eV	$E_{(HOMO)}$[a] vac/eV	$E_{(LUMO)}$[a] vac/eV	$\Delta E_{(HO-LU)}$[b] vac/eV	Oscillator strength[c]
4a	−6.0781	−3.4612	2.6168	0.0302	−6.1397	−3.3594	2.7803	1.1667
4b	−6.1046	−3.5482	2.5563	0.0553	−6.2070	−3.4896	2.7174	1.3016
4c	−6.3208	−3.7033	2.6174	0.1273	−6.3722	−3.6730	2.6992	1.0981
5a	−5.9844	−3.4685	2.5158	0.0397	−5.9577	−3.3040	2.6537	1.5112
5b	−5.9855	−3.4740	2.5115	0.0288	−5.9996	−3.3589	2.6407	1.5117
5c	−6.0662	−3.6591	2.4072	0.0639	−6.2373	−3.6707	2.5667	1.5207

[a] Calculated by DFT using the B3LYP functional and the 6-311 + G(2d,2p) basis set.
[b] $\Delta E = E_{LUMO} - E_{HOMO}$.
[c] Oscillator strength of the transition in DMF, averaged over the eight possible isomers.

Gaussian 09 program [18] using Density Functional Theory (DFT) with the B3LYP functional and various basis sets.

We performed three sets of calculations. In the first set we analyzed the ground state molecular geometry, the ground state energy and the HOMO–LUMO gap for the different isomers by DFT using the B3LYP functional and the 6-311 + G(2d,2p) basis set. All calculations were done for isolated molecules in vacuo and in DMF. For modeling the solvent, a Polarizable Continuum Model (PCM) using the integral equation formalism variant (IEFPCM) was utilized which is the default in Gaussian 09. In the second set of calculations the vertical transition energies for these ground state geometries and the corresponding oscillator strengths were calculated using the same method and basis set with Time Dependent DFT (TDDFT) by inclusion of the 6 lowest excited states: td = (nstates = 6). As an example, the results for the 8 isomers of compound **4a** in DMF are given in Table S1 in the supplementary information. Results for all of the isomeric forms of the other structures can also be found in there.

In Table 4, the values obtained by averaging over the different isomers for each compound is given. A comparison with the experimental HOMO–LUMO gaps obtained from the cyclic voltammetry (Table 1) indicates that the calculated values are roughly 0.6 eV larger. This difference is primarily due to an underestimation of the HOMO energy, which is around 0.7 eV more negative compared to the voltammetric measurements, while the calculated LUMO energies are approximately 0.1 eV more negative than the experimental measurements. This situation is similar to results obtained for recently investigated thienylpyrrole azo dyes bearing benzothiazole groups [3c]. Interestingly the theoretical values differ more from the experimental values for compounds **4** than for derivatives **5** although these include an extra benzene ring.

Although the calculated oscillator strengths for azo dyes **5**, with their extra benzene ring in the π-conjugate bridge are significantly higher, this difference is not reflected in the measured hyperpolarizability values (Table 3). Instead the main trend observed in the measured values is a reduction in the dc limit hyperpolarizability for compounds **5** due to a slight shift of the absorption maximum to the red presumably due to the increase in the length of the π-conjugated bridge.

In a third set of calculations, the activation energies for the respective isomerizations were computed. Only isomerizations around one bond at a time were considered. A first optimization was done assuming a geometry rotated by 90° with respect to the ground state geometry around one of the three isomerizable bonds and with all the other internal coordinates variable for optimization. Using the approximate transition state coordinates obtained from this calculation, a transition state optimization employing the *Synchronous Transit-Guided Quasi-Newton* (STQN) algorithm [19] was employed.

The calculations were done using B3LYP/6-31 + G(d,p) and the option opt = QST3. The resulting transition state energies were compared with the equilibrium structures calculated with the same level of theory. The energy range of isomerization barriers for all calculations can be found in the supplementary information. To summarize, the range for the single barrier crossings range from around 3 to 18 kcal/mol. The conversion rate k is given by simple kinetic theory as $k = A(T)\exp(-\Delta E/kT)$. Assuming a preexponential for an elementary reaction of $A(T) = 10^{13}$ s^{-1} and the highest calculated isomerization barrier of 18 kcal/mol, one gets a lifetime for the corresponding isomer of 0.5 s at 298 K. Even with a smaller value for the pre-exponential, for example due to some concerted mechanism, room temperature thermal energies are sufficient to access all of the possible isomeric forms. Although the solvent model employed does not account for solvent friction, the barriers are probably not much influenced by a low viscosity solvent such as DMF.

Preliminary computational work was also done for calculation of the hyperpolarizabilites of the compounds. As a general observation, the calculated DC hyperpolarizabilities are up to a factor of four lower compared to the frequency dependent hyperpolarizabilities at the second harmonic wavelength of 532 nm. This is strongly indicative of close resonance at the second harmonic of the scattering wavelength and consequently of a strong slope of the hyperpolarizability function. Furthermore DC as well as frequency dependent hyperpolarizabilities vary by a factor of more than 3 between different isomers, although the HOMO, LUMO and oscillator strength values remain nearly constant. This suggests that the statistical distribution amongst isomers could dramatically affect the values of the measured hyperpolarizabilties.

3. Conclusions

We have synthesized two new series of azo dyes, based on bithiophene as donors and simultaneously as π-conjugated bridges and thiadiazolyl and arylthiadiazolyl diazene acceptor moieties. The new compounds were synthesized from commercially available bithiophene and (hetero)aromatic amines. Simple work-up procedures produce fair to moderate yields of these derivatives.

Extensive characterization of the optical (linear and nonlinear) redox and thermal properties was carried out. Experimental hyper-Rayleigh scattering measurements report good β values for these heterocyclic azo dyes with the best values obtained for push–pull derivatives **4c** and **5c** for an incident wavelength of 1064 nm.

Using the simple two-level model to extrapolate to the zero frequency limit, chromophores **4** studied here have hyperpolarizabilities that range from 29% to 37% of the apparent limit identified by Kuzyk [20] while those of series **5** display a normalized response that is between 11% and 15% of the apparent limit for the DC hyperpolarizability. The fundamental model of Kuzyk would predict that by adding six effective electrons contributed by the benzene ring to the π-conjugate bridge, the NLO response of compounds **5** should increase by a factor of $1.7 = (20/14)^{3/2}$. Instead

only a small shift of the absorption peak to the red is observed without any increase in the NLO response.

The theoretical calculations on basis of DFT reproduce the experimental values relatively well. The largest deviation is an underestimation of the HOMO energy, which is around 0.7 eV more negative compared to experiment, similar to previous work.

For the first time we have considered the presence of different isomers due to rotation around three single bonds within the conjugated system, and showed by computation of the transition state energy that indeed all isomers are accessible at room temperature. Furthermore the ground state energies of the different species are almost identical. That leads to the conclusion that the isomers are present in thermal equilibrium in equal concentration. Although the linear absorption parameters such has HOMO and LUMO energies and absorption wavelength varied only marginally between the different isomers, the calculated hyperpolarizabilities, varied by a factor of three. This may explain in part why it is typically very difficult to theoretically estimate the first hyperpolarizabilties of large heterocycle compounds to better than a factor of two in solution.

4. Experimental

4.1. Materials

1,3,4-Thiadiazol-2-amine, 2-amino-5-bromo-1,3,4-thiadiazole, 2-amino-5-(trifluoromethyl)-1,3,4-thiadiazole, 2-amino-5-phenyl-1,3,4-thiadiazole, 2-amino-5-(4-fluorophenyl)-1,3,4-thiadiazole and 2-amino-5-(4-nitrophenyl)-1,3,4-thiadiazole were used as precursors for the synthesis of heterocyclic diazonium salts **2**–**3** and 2,2-bithiophene **1** were purchased from Aldrich and Fluka and used as received.

TLC analyses were carried out on 0.25 mm thick precoated silica plates (Merck Fertigplatten Kieselgel 60F_{254}) and spots were visualized under UV light. Chromatography on silica gel was carried out on Merck Kieselgel (230–240 mesh).

4.2. Synthesis

*4.2.1. General procedure for the azo coupling of bithiophenes **1** with thiadiazole **2a**–**c** and arylthiadiazole **3a**–**c** diazonium salts to afford azo dyes **4a**–**c** and **5a**–**c***

4.2.1.1. Diazotation of 2-amino-1,3,4-thiadiazole, 2-amino-5-bromo-1,3,4-thiadiazole, 2-amino-5-(trifluoromethyl)-1,3,4-thiadiazole, 2-amino-5-phenyl-1,3,4-thiadiazole, 2-amino-5-(4-fluorophenyl)-1,3,4-thiadiazole and 2-amino-5-(4-nitrophenyl)-1,3,4-thiadiazole. Heteroaromatic amines (1.0 mmol) were dissolved in HCl 6 N (1 mL) at 0–5 °C. A mixture of $NaNO_2$ (1.0 mmol) in water (2 mL) was slowly added to the well-stirred mixture of the thiazole solution at 0–5 °C. The reaction mixture was stirred for 10 min at 0–5 °C.

*4.2.1.2. Coupling reaction with bithiophenes **1**.* The diazonium salt solution previously prepared (1.0 mmol) was added dropwise to the solution of bithiophene **1** (0.52 mmol) in acetonitrile (10 mL) and 2–3 drops of acetic acid. The combined solution was maintained at 0 °C for 1–2 h while stirred and then diluted with chloroform (20 mL), washed with water and dried with anhydrous $MgSO_4$. The dried organic solution was evaporated and the remaining azo dyes purified by column chromatography on silica with dichoromethane/*n*-hexane as eluent.

*4.2.1.2.1. (E)-2-(2,2′-bithiophen-5-yldiazenyl)-1,3,4-thiadiazole (**4a**).* Dark pink solid (41 mg, 16%). Mp 166–167 °C. ^{1}H NMR ($CDCl_3$) δ 7.13 (dd, 1H, J = 5 and 3.7 Hz, 4″-H), 7.37 (d, 1H, J = 4.4 Hz, 4′-H), 7.46 (dd, 1H, J = 5.0 and 1.2 Hz, 5″-H), 7.48 (dd, 1H, J = 3.7 and 1.2 Hz, 3″-H), 7.90 (d, 1H, J = 4.4 Hz, 3′-H), 9.08 (s, 1H, 5-H), ^{13}C NMR ($CDCl_3$) δ 124.9, 127.3, 128.5, 128.8, 136.5, 138.7, 147.0, 151.9, 156.1, 179.1. λ_{max} (Dioxane)/nm 475 (ε/dm^3 mol^{-1} cm^{-1} 19,980). IR (Liquid film): ν 3078, 2385, 1524, 1497, 1448, 1341, 1222, 1206, 1189, 1151, 1045, 846, 724 cm^{-1}. MS (EITOF) m/z (%) = 278 ([M]$^+$, 13), 251 (18), 223 (79), 179 (13), 177 (12), 165 (29), 146 (13), 127 (40), 121 (100), 96 (8). HMRS: m/z (EITOF) for $C_{10}H_6N_4S_3$; calcd 277.9755; found: 277.9757.

*4.2.1.2.2. (E)-2-(2,2′-bithiophen-5-yldiazenyl)-5-bromo-1,3,4-thiadiazole (**4b**).* Dark brown solid (41 mg, 21%). Mp 196–197 °C. ^{1}H NMR ($CDCl_3$) δ 7.13 (dd, 1H, J = 5.0 and 3.6 Hz, 4″-H), 7.37 (d, 1H, J = 4.4 Hz, 4′-H), 7.47 (dd, 1H, J = 5.0 and 1.2 Hz, 5″-H), 7.49 (dd, 1H, J = 3.6 and 1.2 Hz, 3″-H), 7.89 (d, 1H, J = 4.4 Hz, 3′-H). ^{13}C NMR ($CDCl_3$) δ 125.2, 127.6, 128.8, 128.9, 136.3, 139.3, 139.9, 147.9, 155.9, 181.2. λ_{max} (Dioxane)/nm 490 (ε/dm^3 mol^{-1} cm^{-1} 36,410). IR (Liquid film): ν 3422, 2718, 1639, 1449, 1368, 848, 811, 701, 545 cm^{-1}. MS (EITOF) m/z (%) = 358 (M^{+81}Br, 7), 356 (M^{+79}Br, 7), 277 (30), 223 (48), 191 (21), 180 (13), 179 (37), 178 (18), 166 (17), 165 (40), 153 (13), 146 (21), 136 (11), 127 (59), 125 (12), 123 (13), 122 (14), 121 (100). HMRS: m/z (EITOF) for $C_{10}H_5^{81}BrN_4S_3$; calcd 357.8839; found: 357.8831.

*4.2.1.2.3. (E)-2-(2,2′-bithiophen-5-yldiazenyl)-5-trifluoromethyl-1,3,4-thiadiazole (**4c**).* Dark pink solid (29 mg, 15%). Mp 180–183 °C. ^{1}H NMR ($CDCl_3$) δ 7.20 (dd, 1H, J = 4.8 and J = 3.3 Hz, 4″-H), 7.48 (d, 1H, J = 5.3 Hz, 4′-H), 7.59–7.61 (m, 2H, 3″-H and 5″-H), 7.86 (d, 1H, J = 5.3 Hz, 3′-H). λ_{max}(Dioxane)/nm 496 (ε/dm^3 mol^{-1} cm^{-1} 28,440) IR ($CHCl_3$): ν 3419, 3100, 3077, 2925, 2359, 1633, 1461, 1450, 1330, 1302, 1262, 1170, 1147, 1100, 1035, 850, 815, 746, 729, 706 cm^{-1}. MS (EITOF) m/z (%) = 346 ([M]$^+$, 17), 330 (16), 250 (24), 223 (38), 192 (17), 179 (12), 178 (30), 177 (15), 165 (31), 161 (25), 149 (54), 146 (16), 127 (40), 127 (38), 123 (24), 121 (100), 112 (30). HMRS: m/z (EITOF) for $C_{11}H_5N_4F_3S_3$; calcd 345.9628; found: 345.9629.

*4.2.1.2.4. (E)-2-(2,2′-bithiophen-5-yldiazenyl)-5-phenyl-1,3,4-thiadiazole (**5a**).* Dark pink solid (60 mg, 58%). Mp 215–217 °C. ^{1}H NMR ($CDCl_3$) δ 7.13 (dd, 1H, J = 4.8 and 3.6 Hz, 4″-H), 7.37 (d, 1H, J = 4.4 Hz, 4′-H), 7.45 (dd, 1H, J = 4.8 and 0.8 Hz, 5″-H), 7.47 (dd, 1H, J = 3.6 and 0.8 Hz, 3″-H), 7.51-7.54 (m, 3H, 3-H, 4-H and 5-H), 7.88 (d, 1H, J = 4.4 Hz, 3′-H), 8.06 (dd, 2H, J = 6.8 and 1.6 Hz, 2- and 6-H). ^{13}C NMR ($CDCl_3$) δ 124.9, 127.2, 128.1, 128.3, 128.7, 129.2, 130.3, 131.7, 136.6, 138.0, 146.6, 156.4, 168.3, 178.3. λ_{max}(Dioxane)/nm 496 (ε/dm^3 mol^{-1} cm^{-1} 23,400). IR (liquid film): ν 3433, 2121, 1640, 1451, 1403, 1330, 1223, 1042, 798, 511 cm^{-1}. MS (EITOF) m/z (%) = 354 ([M]$^+$, 11), 296 (14), 223 (40), 180 (17), 179 (28), 178 (14), 177 (79), 153 (12), 148 (12), 146 (10), 136 (12), 135 (14), 127 (38), 122 (13), 121 (100), 104 (28), 103 (21), 77 (12), 74 (45). HMRS: m/z (EITOF) for $C_{16}H_{10}N_4S_3$; calcd 354.0068; found: 354.0069.

*4.2.1.2.5. (E)-2-(2,2′-bithiophen-5-yldiazenyl)-5-(4-fluorophenyl)-1,3,4-thiadiazole (**5b**).* Dark pink solid (53 mg, 53%). Mp 220–221 °C. ^{1}H NMR ($CDCl_3$) δ 7.14 (t, 2H, J = 8.4 Hz, 3-H and 5-H), 7.16–7.18 (m, 1H, 4″-H), 7.28 (dd, 1H, J = 3.6 and 1.2 Hz, 3″-H), 7.44 (d, 1H, J = 5.4 Hz, 4′-H), 7.54 (dd, 1H, J = 5.2 and 1.2 Hz, 5″-H), 7.81 (d, 1H, J = 5.4 Hz, 3′-H), 7.91 (dd, 2H, J = 7.2 and 5.2 Hz, 2-H and 6-H). ^{13}C NMR ($CDCl_3$) δ 116.3 (d, J = 21 Hz, C3 and C5), 126.3 (d, J = 7.0 Hz, C2 and C6), 127.9, 128.5, 129.0, 129.9, 130.0, 130.1, 130.3, 132.3, 136.3, 161.5, 164.3 (d, J = 251 Hz, C4), 167.0. λ_{max}(Dioxane)/nm 498 (ε/dm^3 mol^{-1} cm^{-1} 36,140). IR (liquid film): ν 3411, 2088, 1640, 1597, 1508, 1449, 1423, 1396, 1326, 1272, 1234,1223, 1191, 1154, 1092, 1062, 1043, 852, 839, 803, 722. 710,672 cm^{-1}. MS (EITOF) m/z (%) = 372 ([M]$^+$, 14), 223 (53), 195 (83), 181 (55), 180 (13), 179 (25), 178 (12), 165 (13), 153 (22), 149 (15), 146 (13), 139 (98), 136 (13), 127 (42), 122 (32), 121 (100), 95 (19), 94 (17), 75 (17), 74 (52). HMRS: m/z (EITOF) for $C_{16}H_9N_4FS_3$; calcd 371.9973; found: 371.9972.

*4.2.1.2.6. (E)-2-(2,2′-bithiophen-5-yldiazenyl)-5-(4-nitrophenyl)-1,3,4-thiadiazole (**5c**).* Dark brown solid (28 mg, 16%). Mp 232–234 °C. ^{1}H NMR ($CDCl_3$) δ 7.20 (dd, 1H, J = 5.2 and 3.6 Hz, 4″-H), 7.29 (dd, 1H, J = 3.6 and 1.2 Hz, 3″-H), 7.48 (d, 1H, J = 5.4 Hz, 4′-

H), 7.58 (dd, 1H, $J = 5.2$ and 1.2 Hz, 5″-H), 7.85 (d, 1H, $J = 5.4$ Hz, 3′-H), 8.10 (dd, 1H, $J = 7.2$ and 2 Hz, 2- and 6-H), 8.32 (dd, 1H, $J = 6.8$ and 2 Hz, 3- and 5-H). ^{13}C NMR ($CDCl_3$) δ 116.2, 116.4, 126.4, 127.9, 128.5, 128.9, 129.8, 129.9, 130.1, 130.3, 132.3, 136.3, 161.5, 163.1, 165.6, 167.0. λ_{max}(Dioxane)/nm 508 (ε/dm^3 mol^{-1} cm^{-1} 12,590). IR (Liquid film): ν 3583, 3087, 1996, 1596, 1560, 1521, 1500, 1459, 1449, 1230, 1420, 1400, 1376, 1351, 1337, 1257, 1221, 1188, 1105, 1048, 988, 916, 897, 870, 860, 780 cm^{-1}. MS (EITOF) m/z (%) = 400 ([M + H]$^+$, 100), 395 (14), 374 (10), 373 (13), 372 (72), 343 (25), 339 (11), 338 (20), 272 (16), 234 (13), 206 (21). HMRS: m/z (EITOF) for $C_{16}H_9N_5O_2S_3$; calcd 399.99911; found: 399.99753.

4.3. Instruments

NMR spectra were obtained on a Varian Unity Plus Spectrometer at an operating frequency of 300 MHz for ^{1}H NMR and 75.4 MHz for ^{13}C NMR or a Bruker Avance III 400 at an operating frequency of 400 MHz for ^{1}H NMR and 100.6 MHz for ^{13}C NMR using the solvent peak as internal reference at 25 °C. All chemical shifts are given in ppm using δ_H $Me_4Si = 0$ ppm as reference and J values are given in Hz. Assignments were made by comparison of chemical shifts, peak multiplicities and J values and were supported by spin decoupling-double resonance and bidimensional heteronuclear HMBC and HMQC correlation techniques. IR spectra were determined on a BOMEM MB 104 spectrophotometer using KBr discs. UV–visible absorption spectra (200–800 nm) were obtained using a Shimadzu UV/2501PC spectrophotometer. Mass spectrometry analyses were performed at the "C.A.C.T.I. -Unidad de Espectrometria de Masas" at the University of Vigo, Spain. Thermogravimetric analysis of samples was carried out using a TGA instrument model Q500 from TA Instruments, under high purity nitrogen supplied at a constant 50 mL min^{-1} flow rate. All samples were subjected to a 20 °C min^{-1} heating rate and were characterized between 25 and 500 °C. All melting points were measured on a Gallenkamp melting point apparatus and are uncorrected. Cyclic voltammetry (CV) was performed using a potentiostat/galvanostat (AUTOLAB/PSTAT 12) with the low current module ECD from ECO-CHEMIE and the data analysis processed by the General Purpose Electrochemical System software package also from ECO-CHEMIE. Three electrode-two compartment cells equipped with vitreous carbon-disc working electrodes, a platinum-wire secondary electrode and a silver-wire pseudo-reference electrode were employed for cyclic voltammetric measurements.

4.4. Solvatochromic study

The solvatochromic study was performed using 10^{-4} M solutions of dyes **4**–**5** and in several solvents at room temperature.

4.5. Nonlinear optical measurements using the hyper-Rayleigh scattering (HRS) method

Hyper-Rayleigh scattering (HRS) was used to measure the first hyperpolarizability β of response of the molecules studied. The experimental set-up for hyper-Rayleigh measurements has previously described in detail [3c]. A Q-switched Nd:YAG laser operating at a 10 Hz repetition rate with approximately 10 mJ of energy per pulse and a pulse duration (FWHM) close to 12 ns is used to excite hyper Rayleigh scattering with an incident wavelength of 1064 nm. The hyper-Rayleigh signal was normalized at each pulse using the second harmonic signal from a 1 mm quartz plate to compensate for fluctuations in the temporal profile of the laser pulses due to longitudinal mode beating. Dioxane was used as a solvent, and the β values were calibrated using a reference solution of *p*-nitroaniline (*p*NA) [15] also dissolved in dioxane at a concentration of 1×10^{-2} mol dm^{-3} (external reference method). The hyperpolarizability of *p*NA dissolved in dioxane is known from EFISH measurements carried out at the same fundamental wavelength. Special care has been taken to use the correct convention [21]. All solutions were filtered (0.2 μm porosity) to avoid spurious signals from suspended impurities. The small hyper Rayleigh signal that arises from dioxane was taken into account. We took particular care to avoid reporting artificially high hyperpolarizibilities due to a possible contamination of the hyper Rayleigh signal by molecular fluorescence near 532 nm. Measurements were carried out using two different interference filters with different transmission pass bands centered near the second harmonic at 532 nm allowing us to estimate and correct for any fluorescence emitted near 532 nm.

Acknowledgments

Thanks are due to the *Fundação para a Ciência e Tecnologia* (Portugal) and FEDER-COMPETE for financial support through the Centro de Química and Centro de Física – Universidade do Minho, Projects PTDC/QUI/66251/2006 (FCOMP-01-0124-FEDER-007429), PTDC/CTM/105597/2008 (FCOMP-01-0124-FEDER-009457), PEst-C/QUI/UI0686/2011 (F-COMP-01-0124-FEDER-022716) and a PhD grant to M. C. R. Castro (SFRH/BD/78037/2011). The NMR spectrometer Bruker Avance III 400 is part of the National NMR Network and was purchased within the framework of the National Program for Scientific Re-equipment, contract REDE/1517/RMN/2005 with funds from POCI 2010 (FEDER) and FCT. The computations were executed on the SeARCH cluster at UMinho (Services and Advanced Research Computing with HTC/HPC clusters), funded by FCT under contract CONC-REEQ/443/EEI/2005.

Appendix A. Supplementary material

Supplementary data associated with this article can be found, in the online version, at doi:10.1016/j.dyepig.2012.05.014.

References

[1] For some examples see: (a) Towns AD. Dyes Pigm 1999;42:3 [and references cited therein];
(b) Metwally MA, Ebrahim A-G, Amira M. Source: Dyes Pigm 2012;92:902.
[2] For some examples see: (a) Yesodha SK, Pillai CKS, Tsutsumi N. Prog Polym Sci 2004;29:45 [and references cited therein];
(b) Matharu A, Jeeva S, Huddleston PR, Ramanujam PS. J Mater Chem 2007;17:4477;
(c) Borbone F, Carella A, Ricciotti L, Tuzi A, Roviello A, Barsella A. Dyes Pigm 2011;88:290;
(d) Mikroyannidis JA, Tsagkournos DV, Balraj P, Sharma GD. J Power Sources 2011;196:4152;
(e) Ábalos T, Moragues M, Royo S, Jiménez D, Martínez-Máñez R, Soto J, et al. Eur J Inorg Chem 2012;76.
[3] (a) Raposo MMM, Sousa AMRC, Fonseca AMC, Kirsch G. Tetrahedron 2005;61:8249;
(b) Coelho PJ, Carvalho LM, Fonseca AMC, Raposo MMM. Tetrahedron Lett 2006;47:3711;
(c) Raposo MMM, Castro MCR, Schellenberg P, Fonseca AMC, Belsley M. Tetrahedron 2011;67:5189;
(d) Raposo MMM, Fonseca AMC, Castro MCR, Belsley M, Cardoso MFS, Carvalho LM, et al. Dyes Pigm 2011;91:62;
(e) Coelho PJ, Castro MCR, Fonseca AMC, Raposo MMM. Dyes Pigm 2012;92:745;
(f) Castro MCR, Fonseca AMC, Belsley M, Raposo MMM. Proc SPIE 2011;8001:80012M1.
[4] (a) Raposo MMM, Ferreira AMFP, Belsley M, Moura JCVP. Tetrahedron 2008;64:5878;
(b) Raposo MMM, Ferreira AMFP, Amaro M, Belsley M, Moura JCVP. Dyes Pigm 2009;83:59;
(c) Coelho PJ, Carvalho LM, Moura JCVP, Raposo MMM. Dyes Pigm 2009;82:130;
(d) Raposo MMM, Castro MCR, Belsley M, Fonseca AMC. Dyes Pigm 2011;91:454.
[5] For some exemples see: (a) Batista RMF, Costa SPG, Malheiro EL, Belsley M, Raposo MMM. Tetrahedron 2007;63:4258;

(b) Batista RMF, Costa SPG, Belsley M, Raposo MMM. Tetrahedron 2007;63:9842;
(c) Batista RMF, Costa SPG, Lodeiro C, Belsley M, Raposo MMM. Tetrahedron 2008;64:9230.
[6] For some examples see: (a) Varanasi PR, Jen AK-Y, Chandrasekhar J, Namboothiri INN, Rathna A. J Am Chem Soc 1996;118:12443;
(b) Albert IDL, Marks TJ, Ratner MA. J Am Chem Soc 1997;119:6575;
(c) Breitung EM, Shu C-F, McMahon RJ. J Am Chem Soc 2000;122:1154;
(d) Hrobárik P, Zahradnik P, Fabian WMF. Phys Chem Chem Phys 2004;6:495;
(e) Zajac M, Hrobárik P, Magdolen P, Foltínová P, Zahradník P. Tetrahedron 2008;64:10605;
(f) Hrobarik P, Sigmundová I, Zahradník P, Kasák P, Arion V, Franz E, et al. Phys Chem C 2010;114:22289;
(g) Kulhanek J, Burés F. Beils J Org Chem 2012;8:25 [and references cited].
[7] (a) Fusco S, Centore R, Riccio P, Quatela A, Stracci G, Archetti G, et al. Polymer 2008;49:86;
(b) Centore R, Fusco S, Peluso A, Capobianco A, Stolte M, Archetti G, et al. Eur J Org Chem 2009;3535.
[8] For some examples see: (a) Hallas G, Choi J-H. Dyes Pigm 1999;42:249;
(b) Yuquan S, Yuxia Z, Zao L, Jianghong W, Ling Q, Shixiong L, et al. Chem Soc Perkin Trans 1999;1:3691;
(c) Ledoux I, Zyss J, Barni E, Barolo C, Diulgheroff N, Quagliotto P, et al. Synth Met 2000;115:213;
(d) He M, Zhou Y, Liu R, Dai J, Cui Y, Zhang T. Dyes Pigm 2009;80:6;
(e) Borbone F, Caruso U, Diana R, Panunzi B, Roviello A, Tingoli M, et al. Org Electron 2009;10:53.
[9] Raposo MMM, Sousa AMRC, Kirsch G, Cardoso P, Belsley M, Matos Gomes E, et al. Org Lett 2006;8:3681.
[10] (a) Herbivo C, Comel A, Fonseca AMC, Kirsch G, Belsley M, Raposo MMM. Dyes Pigm 2010;86:217;
(b) O'Connor MJ, Yelle RB, Linz TM, Haley MM. C R Chim 2009;12:385;
(c) Fitzner R, Reinold E, Mishra A, Mena-Osteritz E, Ziehlke H, Korner C, et al. Adv Funct Mater 2011;21:897.
[11] Mubarak MS, Peters DG. J Electroanal Chem 2001;507:110.
[12] (a) Kamlet MJ, Abboud J-LM, Abraham MH, Taft RW. J Org Chem 1983;48:2877;
(b) Kamlet MJ, Abboud J-LM, Abraham MH, Taft RW. J Am Chem Soc 1977;99:6027.
[13] (a) Clays K, Persoons A. Rev Sci Instrum 1992;63:3285;
(b) Clays K, Persoons A. Phys Rev Lett 1991;66:2980.
[14] (a) Teng CC, Garito AF. Phys Rev B 1983;28:6766;
(b) Stahelin M, Burland DM, Rice JE. Chem Phys Lett 1992;191:245.
[15] (a) Oudar JL. J Chem Phys 1977;67:446;
(b) Oudar JL, Chemla DS. J Chem Phys 1977;66:2664;
(c) Zyss J, Oudar JL. Phys Rev A 1982;26:2016.
[16] Kinnibrugh T, Bhattacharjee S, Sullivan P, Isborn C, Robinson BH, Eichinger BE. J Phys Chem B 2006;110:13512.
[17] Suponitsky KY, Masunov AE, Antipin MY. Mendeleev Comm 2008;18:265.
[18] Frisch MJ, Trucks GW, Schlegel HB, Scuseria GE, Robb MA, Cheeseman JR, et al. Gaussian 09, revision A.1. Wallingford, CT: Gaussian Inc; 2009.
[19] Peng CY, Schlegel HB. Isr J Chem 1993;33:449.
[20] Kuzyk MG. IEEE J Selected Top Quantum Electronics 2001;7:774.
[21] Reis H. J Chem Phys 2006;125:014506.